반도체 접촉장벽 특성의 컴퓨터 해석(I)

論 文
32～6～3

Computer Analysis of Semiconductor Barrier Characteristics(I)

朴 鍾 佑*·黃 金 燦*·朴 昌 燁**
(Jong-Woo Park · Keum-Chan Whang · Chang-Yub Park)

요 약

본 논문은 단일형태의 전하반송자를 포함하여, 단일 접합 (금속—반도체)소자를 기술하는 기본 반도체의 일차원 전송방정식의 정상상태의 전산해를 제시하였다. 전산과정은 "슈팅방법 (shooting method)"에 의하여 간편하게 구하였다. 해석적인 방법에 의하여 완전히 해결하기 어려운 문제인, 공간전하에 분포된 자유반송자를 충분히 고려하여 에너지의 계산, 거리의 함수에 의한 밀도윤곽과 전압—전류의 관계가 제시하였다. 본 논문에서, 그 완전한 해를 통상적인 해와 비교해 볼때, 몇몇 경우에는 통상적인 결과의 오류가 지적되었다.

Abstract

This paper presents a steady-state computer solution of the fundamental semiconductor one-dimensional transport equations, describing a single (metal-semiconductor) contact device, involving only one type of charge carrier. The computations are conveniently made by the "shooting method". A computation of energy, concentration contour as a function of distance and voltage-current relationships are presented, taking full account of free carrier distributed space charges, a problem which is totally inaccessible by analytic means. The misleading of the conventional results in some circumstances are indicated by comparing the exact solutions and the conventional ones in this paper.

I. Introduction

Metal-semiconductor contacts have been studied extensively since the 1930s, after the discovery of their rectifying effects. However, the understanding of transport theory related to rectification phenomena developed only slowly, owing to the complex nature of the results obtained by numerous investigators. For instance, despite the widespread belief that all Schottky barrier transport problems have been solved years ago, there are other problems in this category[1]. In fact, only simplified models

* 正會員：延世大 大學院 電氣工學科
** 正會員：延世大 工大 電氣工學科 教授·工博
接受日字：1983年 2月 26日

have been solved, and in the light of wider experience, it is now known that many of the simplifications involved lead to inadequate representations of the facts. Therefore we have computer procedure, namely complete equations can be solved by computer. A beginning has been made in this direction by the work of Macdonald[2] and Moreau et. al.[3] who both used a "finite system" approach. The present work is further contribution, dealing specifically with contact on materials of low conductivity, in which the bulk region in series with the barrier makes a substantial contribution to system behavior. Accordingly, the present treatment yields results which differ from those of the conventional Schottky model. In this point of view, the objective of this paper was formulated: the classification of exact relationship (energy, concentration contour and voltage-current characteristics) for the single barrier on a semi-infinite bulk.

2. Basic transport equations

The general transport relations consist of two equations for electrons and hole currents, two continuity equations, the Poisson's equation and, of course, suitable boundary conditions. The present treatment is intended to apply to single carrier systems only, and, in the first instance, systems without traps (though traps could easily be introduced) and tunneling effect etc.. Under these condition, the transport equations in one-dimension reduce to

$$j=j_n=eD_n\left[\frac{en(x)E}{kT}+\left(\frac{dn}{dx}\right)\right] \tag{1}$$

$$\frac{dj_n}{dx}=0 \tag{2}$$

$$\left(\frac{dE}{dx}\right)=\frac{\rho(x)}{\varepsilon}=\frac{e[n_d^+-n(x)]}{\varepsilon} \tag{3}$$

where the symbols have their usual meanings. Strictly speaking, Einstein's relationship, which has been used in Eq.(1), is valid only for small concentration gradients, but there is experimental evidence of the fact that its use is justified as long as the current densities involved are not too large.[4]

The computer analysis is most conveniently carried out in terms of normalized equations. All concentrations are normalized to $n(0)$. Other normalizations are as follows (normalized quantities identified as such by bars).

$$\bar{E}(0)=\frac{E}{\left(\frac{kT}{eL_b}\right)},\quad \bar{X}=\frac{X}{L_D},\quad \bar{J}=\frac{jL_D}{eD_n n(0)},$$

$$\bar{N}=\frac{n(x)}{n(0)},\quad \bar{N}_D=\frac{n_d}{n(0)}$$

where L_D is the Debye length, $L_D=\left[\frac{\epsilon kT}{e^2 n(0)}\right]^{1/2}$.

With these definitions, the normalized forms of Eq.(1) and (3) become

$$\bar{J}=\bar{N}(X)E(X)+\frac{d\bar{N}(X)}{dX} \tag{4}$$

$$\frac{d\bar{E}(X)}{dX}=\bar{N}_D-\bar{N}(X) \tag{5}$$

The set of normalized equations may be expressed as two equations, each involving only $\bar{E}(X)$ and $\bar{N}(X)$, but it is important to be able to seperate the variables. With this objective, Eq.(4) may be written as

$$\bar{E}(X)=\frac{1}{\bar{N}(X)}\left[\bar{J}-\frac{d\bar{N}(X)}{d\bar{X}}\right] \tag{6}$$

and Poisson's equations (5) may be re-written by substituting (6) into (5)

$$\frac{d^2\bar{N}(X)}{dX^2}=\bar{N}(X)\left[\bar{N}(X)-\bar{N}_D\right]-\frac{d\bar{N}(X)}{d\bar{X}}\left[\bar{J}-\frac{d\bar{N}(X)}{d\bar{X}}\right]\frac{1}{\bar{N}(X)} \tag{7}$$

This is the key equation of the present work, and all the results presented are derived from it by numerical solutions. In order to get solutions,

based on a modified Euler's formulation, a form of the shootting method was used.

In the present model, the barrier height was taken as 20kT. It is an arbitrary figurer, adopted only for plotting purposes. The calculations are in no way concerned with it, because it denotes the barrier height as seen from the metal. In contrast, our calculations deal only with what goes on inside the semi conductor which means that the kind of metal is unimportant. In practice, the barrier height as seen from the metal might be different from 20kT, and this would certainly change the boundary concentration $n(0)$. It doesn't matter because all calculations are in terms of the ratio $n(x)/n(0)$. Of course, it would have been possible to normalize the concentrations with reference to n_{∞}, rather than $n(0)$. That choice is arbitrary. In any practical case, $n(x)=n(0)$. $\bar{N}(x)$, where $\bar{N}(x)$ is computer result, and $n(0)$ is whatever actual boundary concentration one wants to adopt.

3. Results

The normalized specimen thickness $\bar{X}_T$ was here taken as 6, through calculations were in fact made for many other thicknesses. From the computer results (energy vs distance), Fig. 1 shows the zero-current energy contours for normalized donor concentrations of 5 and 10. The corresponding diffusion potentials evaluated by the program turn out to be 1.63 and 2.33 respectively and these values are very close to expectation from Boltzmann

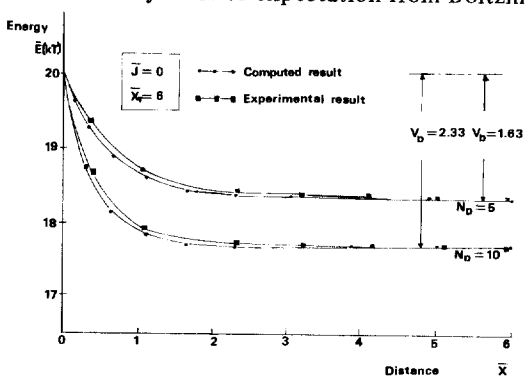

Fig. 1. Energy-distance dependence for zero-current $\bar{J}=0$, $\bar{X}_T=6$, $\bar{N}_D=5, 10$

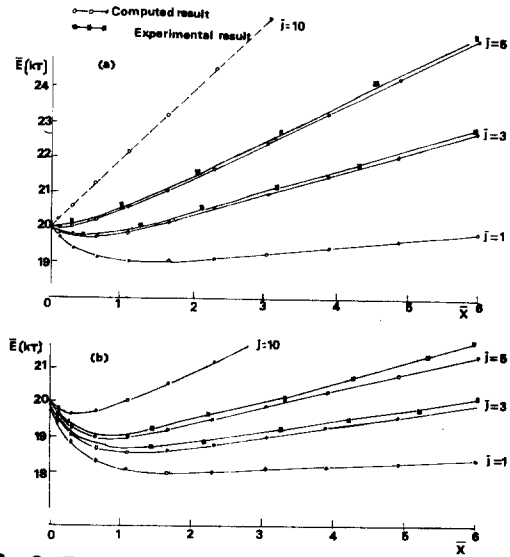

Fig. 2. Dependence of barrier profile on distance for various forward current values.
(a) $\bar{N}_D=5$, $\bar{X}=6$, $\bar{J}=1,3,5,10$ *and*
(b) $\bar{N}_D=10$, $\bar{X}_R=6$, $\bar{J}=1,3,5,10$

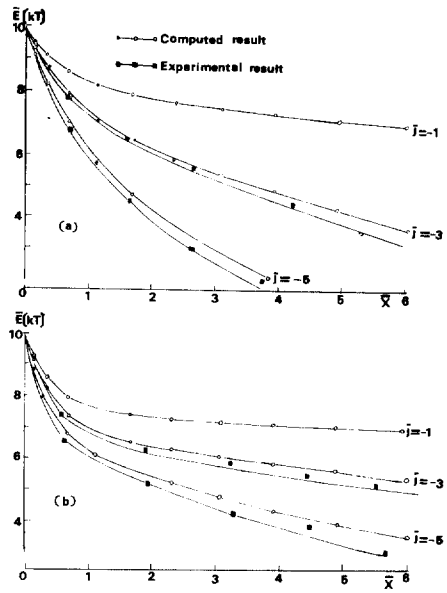

Fig. 3. Dependence of barrier profile on distance for various reverse current values.
(a) $\bar{N}_D=5$, $\bar{X}_T=6$, $\bar{J}=-1, -3, -5$
(b) $\bar{N}_D=10$, $\bar{X}_T=6$, $\bar{J}=-1, -3, -5$

statistics. In fact, exp (1.63)=5.10 and exp (2.33)= 10.27, when used as $N_D=5$ and 10, would imply diffusion potentials of 1.61 and 2.31 respectively. However, it must be remembered that the exponential function is particularly

sensitive to error in the argument, and the "target" of the shooting method is "hit" only with an accuracy of about 1%. The results are therefore entirely consistant. Greater accuracy could be obtained at any time if it were needed, but in practice, diffusion potentials cannot be determinde with greater precision from contact measurements. Fig. 2 and 3 give corresponding results in the presence of forward and reverse currents. The reality of the voltage drop which occurs across the bulk material is clearly seen, and so is the fact that the bulk fields for equal and opposite currents are equal and opposite, as of course they must be. In the conventional model, all these slopes are regarded as zero. At all these points, the current is carried entirely by diffusion. The fact that the curvature of the contours extends beyond the minima demonstrates that diffusion currents remain significant over some distance in the bulk. In the reverse direction, there are no energy minima, of course.

At forward current density slightly greater than 5(for $\bar{N}_D$=5), the barrier is evidently eliminated ("flat-band condition"), as shown by Fig. 2. Higher values of $\bar{N}_D$ call for higher currents to achieve the same results.

Fig. 4 gives carrier concentration profiles, and demonstrates, amongst other things, that concentration gradients increase in the forward and decrease in the reverse direction of current flow. Accordingly, diffusion is the principal mechanism for sustaining forward current and drift for sustaining reverse current. When net current is zero, drift and diffusion are precisely balanced.

Under the forward direction, two kinds of "applied voltages" are of interest in the present results, namely V_a which is across the barrier itself, and V_{XT} which is across the system as a whole. In the conventional model, the potential difference does not appear because the bulk region is regarded as flat everywhere.

Fig. 5 shows how the I-V_a and I-V_{XT} characteristics depend on donor concentrations for $\bar{X}_T$=6 in the

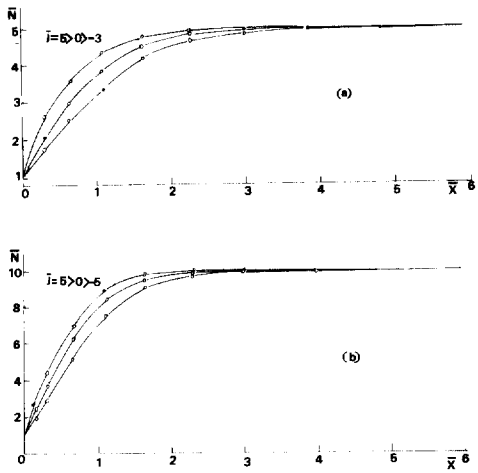

Fig. 4. Distance dependence of carrier concentration for various current values.
(a) $\bar{N}_D$=5, $\bar{X}_r$=6 *and*
(b) $\bar{N}_D$=10, $\bar{X}_r$=6

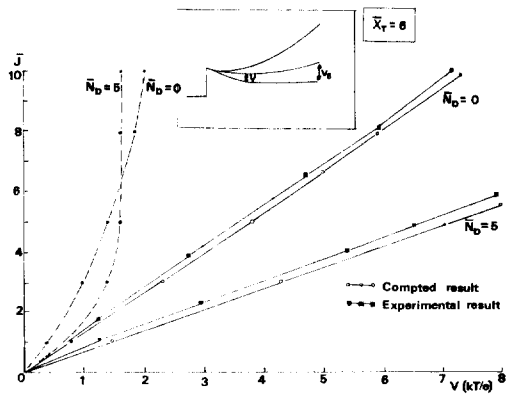

Fig. 5. $\bar{J}$-V_a (dotted line) and $\bar{J}$-V_a(solid line) characteristics under forward-bias. $\bar{X}_r$=6, $\bar{N}_D$= 5, 10.

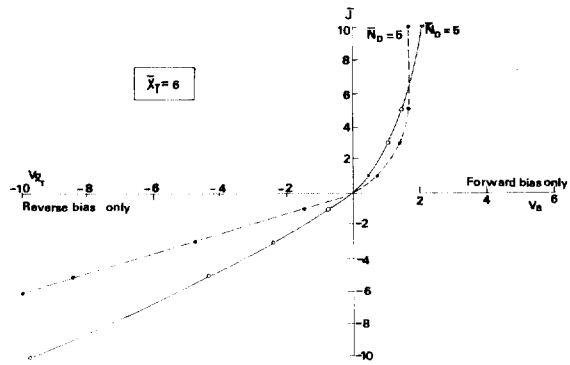

Fig. 6. $\bar{J}$-V characteristics for normalized donor concentration. $\bar{X}_r$=6, $\bar{N}_D$=5 (dotted line), $\bar{N}_D$=10 (solid line).

forward direction .

V_a is not an operational entity, since only V_{XT} is accessible to direct measurement. V_a is therefore interesting only for the purpose of comparsion with conventional theory. As the barrier thickness is reduced from 6 to 1, the I-V_{XT} curves get gradually close to the I-V_a curves, as of course, they must. In the reverse direction, there is no V_a, because no zero-electric field point exists. Complete I-V characteristics is given in Fig. 6.

All experiments for energy contours and I-V characteristics were carried out by simple single-probe measurement.

4. Discussion of results

On the basis of the exact computer results for the single barrier, the following conclusions can be drawn: (1) Normalized current in Schottky theory can be obtained as follows;

$$\bar{J}=\left[\frac{\bar{V}_D+\bar{V}_B}{\bar{V}_B}\right]^{\frac{1}{2}} \quad [\,1-\exp(-\bar{V}_B)\,] \qquad (8)$$

where $\bar{J}$=normalized current in Schottky theory,

$$\bar{J}=\frac{J}{\sigma\left[\frac{8\pi Ne}{k}\right]^{\frac{1}{2}}\left[\frac{kT}{e}\right]^{\frac{1}{2}}[V_D]^{\frac{1}{2}}}=\frac{J}{J_0},$$

$$\bar{V}_D=\frac{eV_D}{kT},\quad \bar{V}_B=\frac{eV_B}{kT}$$

Schottky theory assumes $eV_D \gg kT$. Here the diffusion potential V_D was quite small, e.g. 2.3kT/e, and the Schottky model is therefore expected to fail. Fig. 7 shows how drastic the fail is. As $\bar{X}_T$ increases, our externally measurable rectification disappears, because the bulk resistace dominates. Of course, rectification based on V_a remains. As $\bar{N}_D$ increases based V_D is also increased, because the higher diffusion potential value can be obtained. The present model then comes closer to the Schottky one.

(2) The shape and thickness of the barrier in the presence of an applied voltage can be found by the use of Poisson's equation. For the conventional Schottky model, one may get a normalized value of the barrier width as follows:

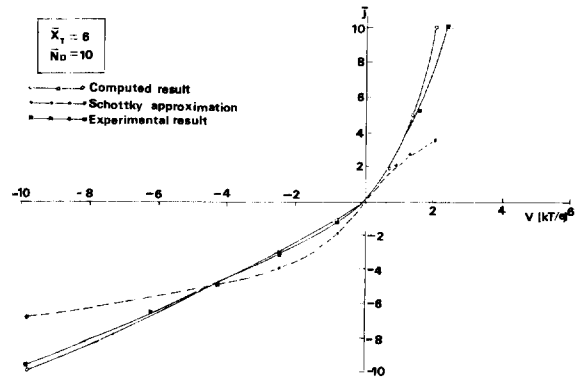

Fig. 7. Comparison of $\bar{J}$-V characteristics computed results the conventional Schottky approximation and the experimental result.
(a) $\bar{X}_r$=6, $\bar{N}_D$=10

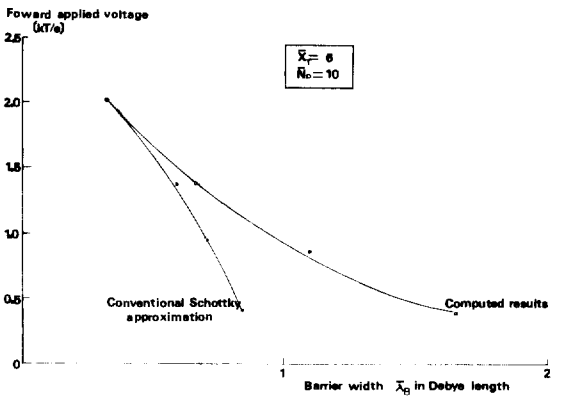

Fig. 8. Comparison barrier width between results and conventional Schottky approximation. $\bar{X}_r$=5, $\bar{N}_D$=10

$$\bar{\lambda}_B=\frac{\bar{V}_B+\bar{V}_D}{\bar{V}_D}$$

where λ_B= normalized barrier thickness.

$$\bar{V}_B=\frac{eV_B}{kT}\quad \bar{V}_D=\frac{eV_D}{kT}$$

V_B is the voltage across the barrier itself as conventionally defined by disregarding the ohmic drop across the bulk. When the free carrier concentration is taken into account, the behavior is entirely different. In Fig. 8, V_B is shown plotted against

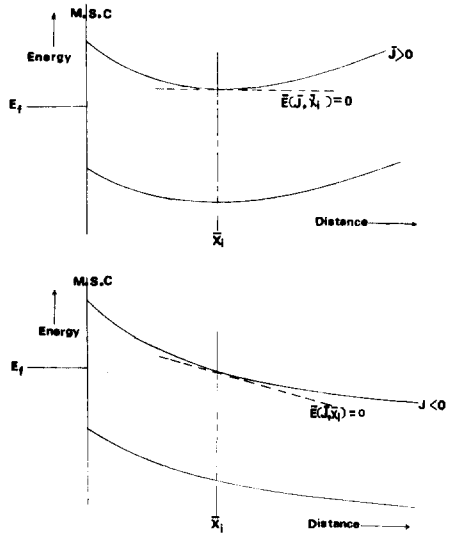

Fig. 9. Energy band diagram of a single barrier in (a) forward direction: a current dependent point X_i can defined at which $\bar{E}(J,X_i)=0$
(b) Reverse direction: the electric field is nonzero at all points.

conventional and computed barrier width for comparison. The physical reason for the discrepancy between the computed and conventional width is straingforward; the presence of free carrier simulates an effectively lower density of donors; hence the greater barrier thickness.

(3) According to the present analysis, the general energy diagram of a single barrier (in the present work) is suggested in Fig. 9.

References

1) H.K. Henisch, personal communication
2) J.R. Macdonald, Solid-State Electronics 5, 11(1962).
3) Y. Moreau, J.C. Manifacier and H.K. Henisch, Solid State Electronics **25**, 133 (1982).
4) Transistor Teacher's Summer School, Phys Rev. **88**, 1368 (1952).